Proceedings of The National Conference
On Undergraduate Research (NCUR) 2015
Eastern Washington University, Cheney, WA
April 16-18, 2015

Complete Kinetic and Mechanistic Decomposition of Zinc Oxalate with Characterization of Intermediates and Final Oxide

Nicholas D. Cooper
Chemistry
James Madison University
800 S Main St, Harrisonburg VA 22807

Faculty Advisor: Thomas C. DeVore

Abstract

Although the thermal decomposition of zinc oxalate was considered to follow a one-step mechanism, newer isoconversional methods indicate that the activation energy is a function of the extent of reaction and of the sample mass. This suggests that the mechanism may actually have several steps. Evolved gas analysis-Fourier transform IR spectroscopy (EGA-FTIR) indicates that the gaseous products, CO and CO_2, are produced at different rates supporting the conclusion from the isoconversional investigations. EGA indicates that CO is formed initially while CO_2 forms later. These results are consistent with the mechanism proposed by Boldyrev.[1] He proposed that the initial step in the mechanism is an oxalate anion rearrangement to produce a carbonate-carbonyl intermediate. This intermediate then loses CO to produce the carbonate. Decomposition of the carbonate then produces the CO_2. No evidence for this intermediate has been found using either X-Ray diffraction or FTIR spectroscopy.

Keywords: Kinetic, Thermal Decomposition, Zinc Oxalate

1. Introduction

Zinc oxide is used for different industrial applications due to its catalytic and light reflectivity properties.[2,3] The thermal decomposition of zinc oxalate has been used to generate very pure fine grain ZnO powder and ZnO nanoparticles for many of these applications.[4,5,6] Although Yankwich and Zavitsanos[7] determined the decomposition was a 4 step process with an activation energy of ~ 200 kJ mol for each step, later researchers have favored this decomposition being a single step process.[8,9,10,11] Since the consensus is that zinc oxalate decomposes in one step without complete melting to produce zinc oxide, carbon dioxide and carbon monoxide at most pressures in inert atmospheres,[12] Aggarwal and Dollimore[8] recommend using it as a thermal decomposition reference standard to calibrate thermal analysis instruments.

However, the value determined for the activation energy of this decomposition has not been established with certainty. The value determined for the activation energy (300 kJ/ mol) by Aggarwal and Dollimore[8] is ~100 kJ/mol larger than the value reported by Yankwich and Zavitsanos, or by Danforth and Dix.[9] The most complete investigation done to date by Malecka, Drozdz-Ciesla, and Malecki[10] was analyzed using the Avrami–Erofe'ev equation with $n \approx 2$ giving an activation energy between 181.4-186.5kJ/ mol for $0.2 < \alpha < 0.8$. A recent model-free analysis by Chengcheng Hu et al[11] reported an activation energy of ~120 kJ/ mol for this decomposition.

Boldyrev has established that the thermal decomposition of metal oxalates fall into three classifications:

A. Those decomposing to produce the metal carbonate and CO
B. Those decomposing to produce the metal oxide, CO and CO_2
C. Those decomposing to produce the metal and CO_2.

The decomposition of zinc oxalate is a member of category B with growing evidence that it follows the mechanism for category A. Based on the investigation of the decomposition of the oxalate ion trapped in salt matrices to produce the carbonate ion as the principle product, Hartman and Hisatsume[13] concluded that the C-C bond in the oxalate brakes producing two CO_2^- ions. These ions then rearranged to produce carbonyl carbonate as a likely intermediate in the process. Support for this mechanism came from the observation of CO_2^- in the ESR spectrum during the thermal decomposition of strontium oxalate by Angelov et al.[14] Recently, Kolezynski and Malecki[15] concluded that the decomposition of the alkali metal oxalates likely goes through this intermediate based on the DFT-FP-LAPW they did for this system further supporting this mechanism.

Boldyrev suggested that the first step in the decomposition of each classification was the breaking of the C-C bond to produce two CO_2^- anions, which could recombine to produce carbonyl carbonate [CO_3CO^{2-}].[1] While electron transfer complicates the mechanism for category C, this could also be a viable mechanism for category B. However, DFT calculations done for zinc oxalate by Kolezynski and Malecki[15] suggest this may not be the case. Their calculations indicate that one of the zinc oxide bonds breaks first leaving a partially anchored oxalate ion. The C-C bond then breaks to produce a CO_2 molecule and the CO_2^{2-} anion which rapidly decomposes to give zinc oxide and CO.

Neither the activation energy nor the decomposition pathway have been established unequivocally for zinc oxalate. Since better knowledge of these could lead to more efficient processes for manufacturing ZnO, the newer more accurate isoconversional methods were used to investigate this decomposition. Thermal gravimetric analysis (TGA) and EGA-FTIR were used identify the gases produced during the reaction and to investigate the dynamics of the process. FTIR and PXRD were used to characterize the solid phases involved in the reaction. Particular attend was paid to the initial decomposition region ($0.2<\alpha$) that was largely ignored in the previous investigations to determine if this region offered addition clues about the decomposition mechanism. These measurements indicated that the apparent activation energy was a function of both the sample mass and the extent of reaction indicating that the reaction followed a multiple step mechanism. EGA-FTIR indicated that there is a slight excess of CO during the initial reaction, supporting the possibility that carbonyl carbonate is an intermediate in the decomposition of classification B compounds. However, no evidence of this intermediate was observed in neither the IR nor the XRD of the solids formed during the decomposition. This result does not support that the conclusion that CO_2 is produced initially as indicated by the DFT calculations. Evidence for these observations are presented below.

2. Experimental

Zinc oxalate was synthesized from the reaction between solid zinc chloride $ZnCl_2$ (Fischer Scientific-ACS certified) and sodium oxalate $Na_2C_2O_4$ (Fischer Scientific-ACS certified). Each salt was dissolved in 25 ml of deionized water and heated to approximately 325 K on a hot plate. The solutions were mixed and stirred in order to ensure homogenous mixture and complete formation of product. The beaker was taken off heat after 15 minutes and allowed to cool. The white precipitate was vacuum filtered and allowed to dry overnight in ambient air.

Thermal gravimetric analysis was done using a Mettler-Toledo TGA/SDTA851^e. Data for model free kinetics were obtained by placing carefully weighed samples in alumina crucibles and heating at rates of 1, 2, 5, 10 15, 20, 25, 30, and 40 K min^{-1} in an atmosphere of 50 ml/ min flowing nitrogen. Sample sizes of 1 mg, 5 mg, and 10 mg were done to determine the effect of sample size on the apparent activation energies. Isothermal kinetics were obtained by heating the sample to the desired temperature at 20 K min^{-1} and allowing it to remain there for 60 minutes. The atmosphere was the same as those used for the non-isothermal measurements.

Evolved gas analysis- Fourier Transform IR was done by placing a home built stainless steel vacuum cell placed in the sample compartment of a Thermo Nicolet 6700 Fourier Transform Infrared Spectrometer. Samples were place in a 9 mm O.D. glass tube with one in sealed. The open end of the tube was connected to the cell using an O-ring connector and the cell was evacuated to a residual pressure of ~ 800 Pa. using a standard vacuum pump. The sample was heated with a furnace constructed by wrapping a quartz tube with nichrome heating wire. The power to the furnace was supplied by a BK Precision High Current Regulated DC Power Supply. The cell could be heated in either isothermal or non-isothermal mode by adjusting the power supplied to the furnace. The temperature was measured with a Fluke $51^{K/J}$ thermometer placed between the sample tube and the furnace. IR Spectra of the evolved gases were obtained at 4 cm^{-1} resolution every 2 seconds for times up to 60 minutes. No carrier gas was used for these experiments since the vacuum pump was used to draw the evolved gases through the cell.

3. Results and Discussion

FTIR and TGA were used to establish that zinc oxalate dehydrate had been synthesized. The IR bands observed in KBr pellets are compared to those reported for zinc oxalate dehydrate by Wladimirsky et al in Table 1.[16] The assignments for each band is also given in Table 1. Agreement within experimental error confirms that zinc oxalate had been synthesized.

Table 1: IR Bands Observed for $ZnC_2O_4 \cdot 2\ H_2O$ in KBr are compared to the values given by Wladimirsky. The assignments for each band are also given in the table.

Observed	**Wladimirsky**	**Assignment**
3377 VS	3383 VS	ν (OH)
3158 SH	3157 SH	ν (OH)
2948 VW	2947 VW	ν (OH)
1629 VS	1632 VS	$\nu_{as}(CO)$
1363 S; 1318 S	1364 S; 1320 S	$\nu_s(CO) + \delta(OCO)$
821 S	823 S	$\nu_s(CC) + \delta(OCO)$
745 m; 617 m	745 m; 618 m	$\rho(H_2O)$
494 s; 456 S	495 S; 456 S	δ_{RING}

The TGA was also consistent with the previously reported patterns. As shown in Figure 1, two main mass loss regions are observed. Infrared spectra were taken after heating the sample to several temperatures and then cooling it back to room temperature. The results are presented in Figure 2. The broad OH peak at 3377 cm^{-1} in the initial compound is no longer observed after heating the sample to 450 K. Since the oxalate bands are still clearly present, this confirms that the waters of hydration are lost in this step. The measured mass loss (18.97%) gives a calculated loss of 1.996 moles of water assuming the compound were 100% pure. The oxalate bands are no longer observed after heating to 700 K confirming that the oxalate decomposed during the second step. The total observed mass loss (57.1%) observed after the second step is slightly larger than the theoretical mass loss of 56.6% assuming ZnO is the only product. Both results indicate that the synthesized $ZnC_2O_4 \cdot 2\ H_2O$ was better than 98% pure.

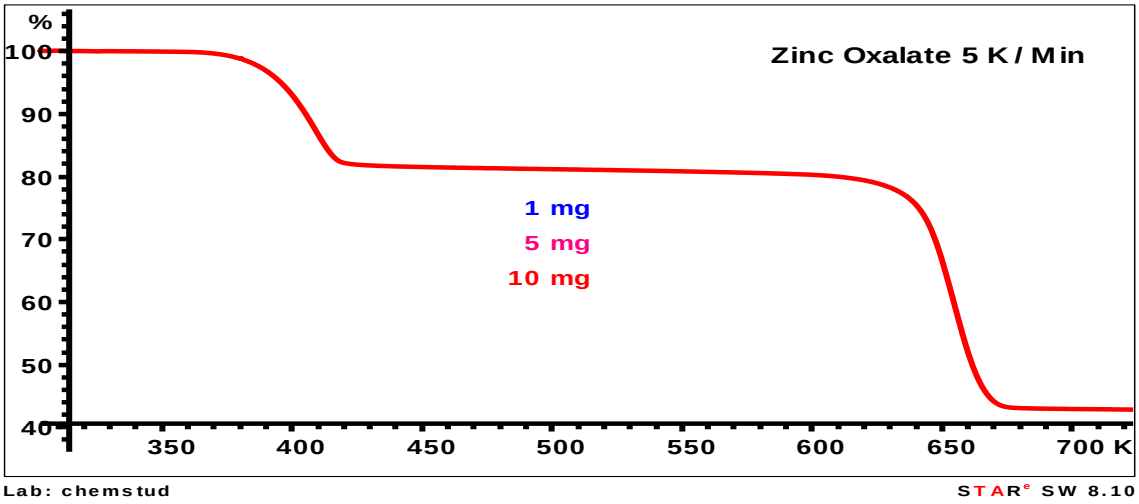

Figure 1: Thermal gravimetric analysis done on 1, 5, and 10mg samples of hydrated zinc oxalate in flowing nitrogen at a heating rate of 5 K min^{-1}.

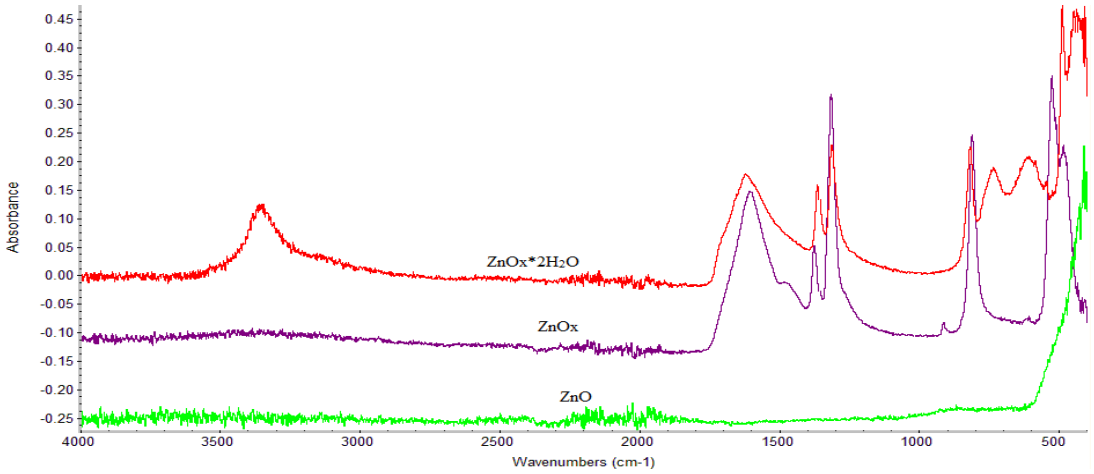

Figure 2: IR data of ZnC_2O_4 as it is decomposed by heating it to 450 K and to 700 K in the TGA.

Isoconversional methods were used to determine the Arrhenius constants for this decomposition. Thermal gravimetric analysis data were collected for 1, 5, and 10mg samples using several heating rates between1 K min^{-1} and 40 K min^{-1}. The measured mass losses were converted to the extent of reaction (α) following the procedure given by Vlaev et al.[17] and the ICTAC Kinetics Committee.[18] The α vs temperature plots obtained for a 10 mg sample are shown in Figure 3. These plots were then used to find the activation energy using the Starink method[19] which uses equation (1).

$$(1)\quad \ln\left(\frac{\beta}{T^{1.92}}\right) = Const. - 1.008\frac{E_A}{8.314T}$$

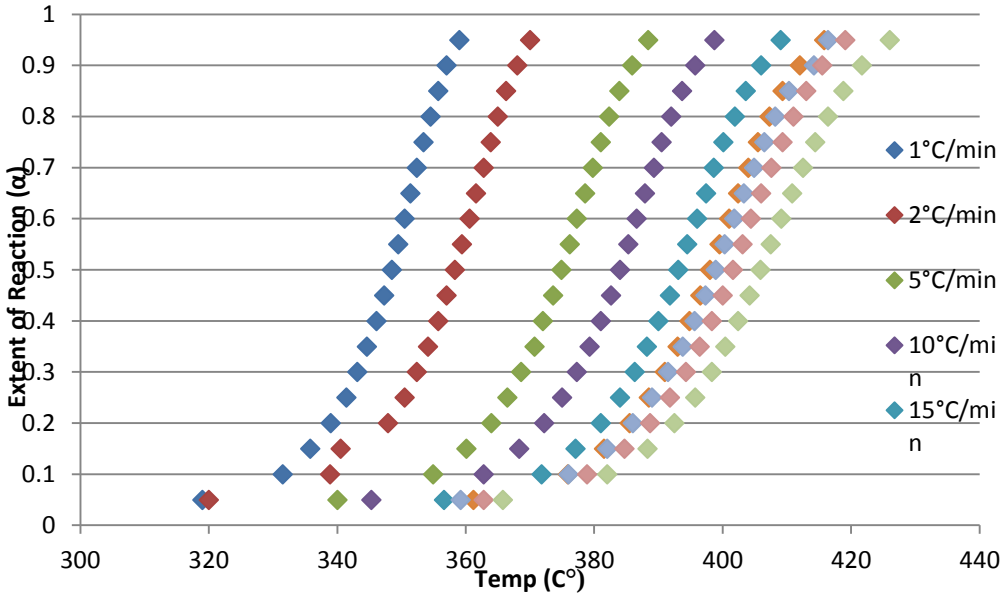

Figure 3: 10mg sample of ZnC_2O_4 ran through TGA at heating rates ranging from 1°C/min to 40°C/min. Extent of reaction (α) was plotted versus temperature in C in order to check the reaction progress over time with differing heating rates.

Plots of $Ln\left(\frac{\beta}{T^{1.92}}\right)$ vs. $1000/T$ were made for 0.05< α < 0.95 and linear least squares were used to determine the slope of the line. The slope is equal to -1.008 E_A/ R where Ea is the activation energy and R is the universal gas constant. An example of these plots is given in Figure 4. The activation energies determined for each sample mass are plotted as a function of α in Figure 5.

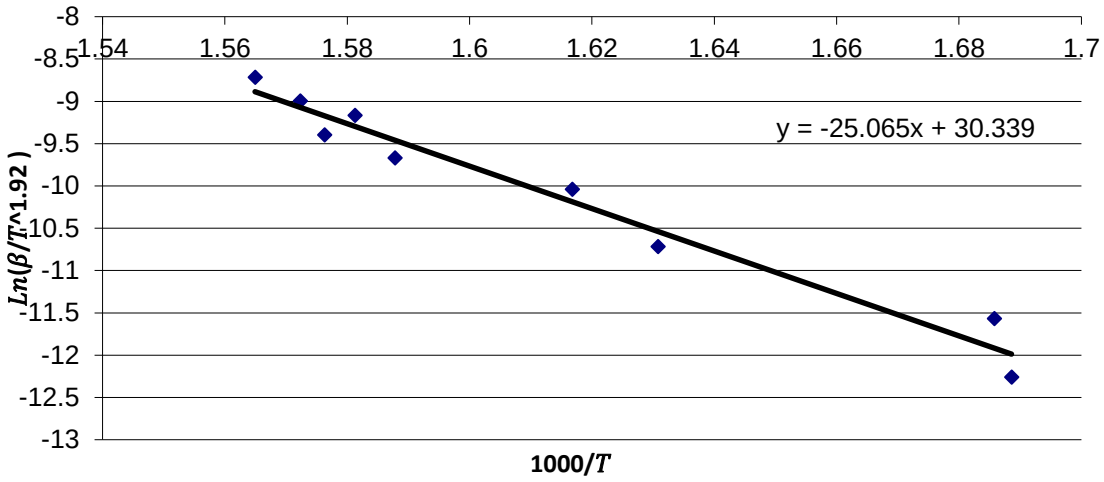

Figure 4: Plotting the isoconversional method calculation using 5mg sample at α=0.4

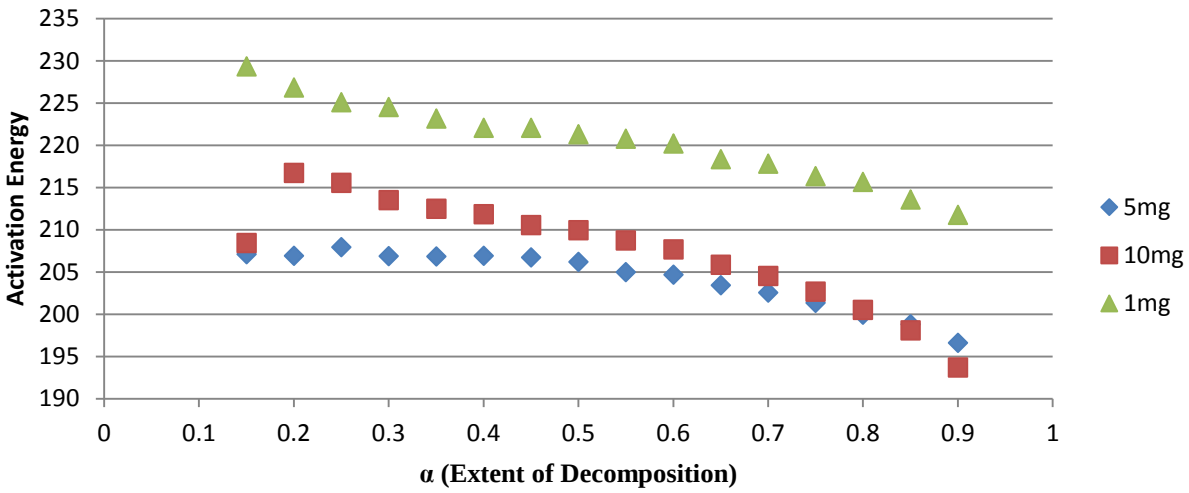

Figure 5: Graph of the activation energy of the decomposition as α increases from 0.15 to 0.90.

It is obvious that the apparent activation energy is both a function of sample mass and the extent of the decomposition. This is clear evidence that this decomposition follows a multiple step mechanism. The trends observed for the activation energies (a decrease for 0.1 < α < 0.35, a plateau for 0.4 < α < 0.55, and a decrease for α> 0.6) are consistent with the trends observed for mechanisms with reversible steps where the rate of the forward reaction decreases as the sample is depleted while the rate of the reverse reaction increases as the partial pressure of the product gases increases in the cell. This effect also explains the sample mass dependence since the rate of transport from the cell usually decreases as the sample size is increased.

Evolved gas analysis provided additional information that this decomposition is following a multi-step mechanism. Figure 6 shows the normalized integrated intensities observed for CO and CO_2 collected in the IR cell as a function

of temperature while the zinc oxalate thermally decomposed. Each data point in this plot was determined by measuring the integrated intensity of each band at each temperature and then dividing it by the integrated intensity determined for complete depletion of the sample. This normalizes the relative amounts of each compound and gives the stoichiometric 1:1 ration expected for CO and CO_2 at the completion of the reaction. This procedure assumes the decomposition reaction is the only one occurring. It does not account for possible secondary reactions such as the disproportionation of CO to form CO_2 and graphite. This data indicates that there is an excess of CO for $\alpha < 0.2$. This suggests that the decomposition may occur through the formation of $ZnCO_3$ as is observed for the alkali and alkaline earth metals. This suggests the same mechanism may be occurring for Boldyrev's Type 1 and type 2 reactions.

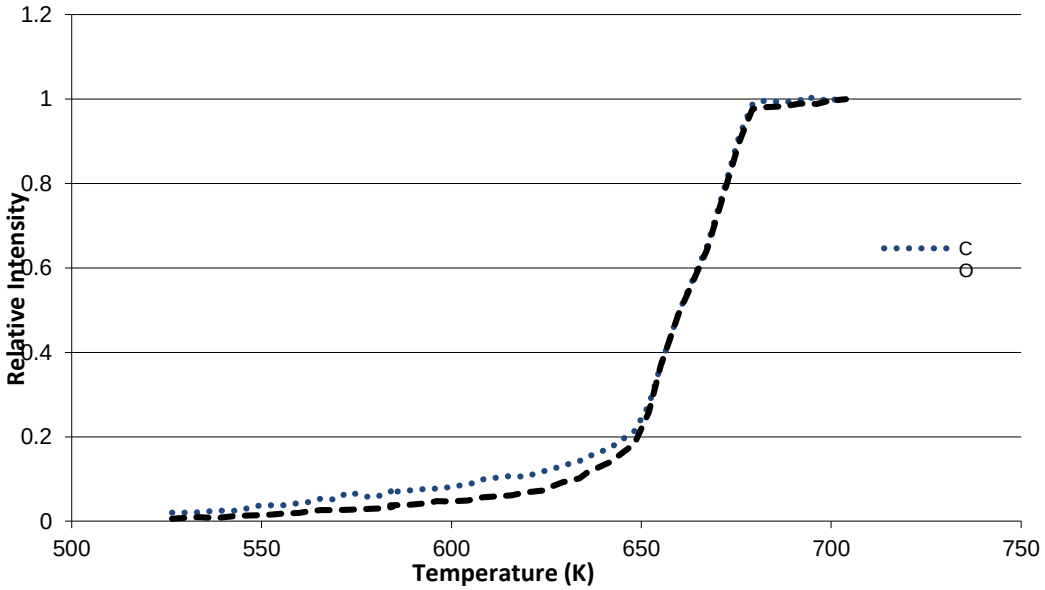

Figure 6: Relative amounts of CO and CO_2 collected in the IR cell as a function of temperature from the thermal decomposition of ZnC_2O_4 assuming the reaction is stoichiometric.

4. Mechanism

Although the thermal decomposition of metal oxalates is generally considered to be an irreversible process, the isoconversional kinetics measurements indicate that there is a least one reversible step in a multi-step mechanism. The EGA-FTIR indicated that CO is formed first. This suggests that the thermal decomposition of zinc oxalate follows a mechanism similar to the one proposed by Boldyrev for the thermal decomposition of silver oxalate.[1] In it, a metal oxygen bond breaks and the "free oxalate" rearranges with the breaking of the C-C bond to form a carbonyl carbonate via a reversible process. This carbonyl carbonate can then lose CO (also probably a reversible process) to leave the carbonate which then thermally decomposes to form CO_2 and the metal oxide. Since some anion mobility is needed, the decomposition likely occurs near the nominal melting point of the metal oxalate. The reaction scheme, only considering the anions, is pictured in Figure 7 with each step in this scheme having the possibility of being reversible.

$$C_2O_4^{2-} \Leftrightarrow [CO_3CO]^{2-}$$

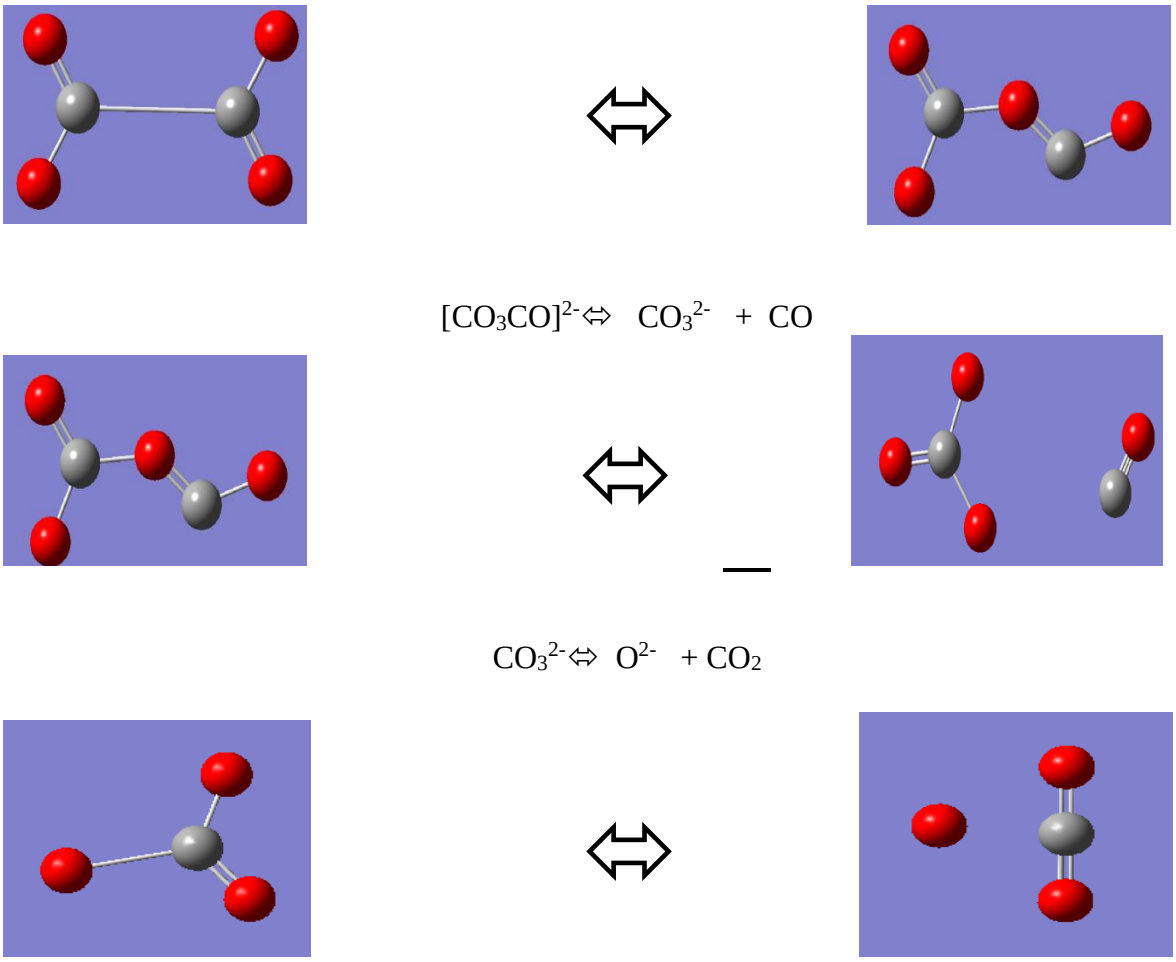

Figure 7: Molecular representation of the decomposition of anhydrous zinc oxlate.

5. Conclusion

Both isoconversional kinetic analysis and the EGA-FTIR of the initial decomposition region indicate that the thermal decomposition of zinc oxalate follows a multi-step mechanism. The EGA-FTIR indicates that CO is formed in excess initially. This result is not consistent with the conclusion that the CO_2 would form initially proposed by Kolezyniski and Malecki based on their analysis of the bond energies determined using DFT calculations, but it is consistent with the clear initial formation of CO exhibited by the category A metals. This suggests that the mechanism proposed for these metals may also be applicable for zinc oxalate. A reaction scheme similar to the one presented by Boldyrev for the thermal decomposition of silver oxalate is proposed that will explain all of these observations. The kinetics for each possible step in this mechanism has not been measured. This will be the focus of future investigations.

6. References

1. Boldyrev, V. V. Thermal decomposition of silver oxalate. *Thermochim Acta* **2002**, *388*, 63-90. DOI10.1016/S0040-6031(02)00044-8

2. Kumar, S.; Verma, N. K.; Singla, M. L. Reflective properties of ZnS nanoparticle coatings. *J. Coat. Tech. Res.* **2011**, *8*, 223-228. DOI10.1007/s11998-010-9290-1.

3. Boemare, C.; Monteiro, T.; Soares, M. J.; Guilherme, J. G.; Alves, E. Photoluminescence studies in ZnO samples. *Phys B Condens Matter* **2001**, *308-310*, 985-988. DOI10.1016/S0921-4526(01)00854-7.

4. Özgür, Ü.; Alivov, Y. I.; Liu, C.; Teke, A.; Reshchikov, M. A.; Doğan, S.; Avrutin, V.; Cho, S. -.; Morkoç, H. A comprehensive review of ZnO materials and devices. *J. Appl. Phys.* **2005**, *98*, 1-103. DOI10.1063/1.1992666.

5. Wang, Z. L. Zinc oxide nanostructures: Growth, properties and applications. *J Phys Condens Matter* **2004**, *16*, R829-R858. DOI10.1088/0953-8984/16/25/R01.

6. Wang, Z. L. Nanostructures of zinc oxide. *Mater. Today* **2004**, *7*, 26-33. DOI10.1016/S1369-7021(04)00286-X.

7. Yankwich, P. E.; Zavitsanos, P. D. Pyrolysis of zinc oxalate: Kinetics and stoichiometry. *J. Phys. Chem.* **1964**, *68*, 457-463.

8. Aggarwal, P.; Dollimore, D. The use of zinc oxalate dihydrate in establishing the working reproducibility of a simultaneous TG-DTA unit. *Instrum Sci Technol* **1996**, *24*, 95-102.

9. Danforth, J. D.; Dix, J. Chemistry and kinetics of the thermal decomposition of zinc and magnesium oxalates. *J. Am. Chem. Soc.* **1971**, *93*, 6843-6846.

10. Malecka, B.; Drozdz-Ciesla, E.; Malecki, A. Mechanism and kinetics of thermal decomposition of zinc oxalate. *Thermochim Acta* **2004**, *423*, 13-18. DOI10.1016/j.tca.2004.04.012.

11. Hu, C.; Mi, J.; Shang, S.; Shangguan, J. The study of thermal decomposition kinetics of zinc oxide formation from zinc oxalate dihydrate. *J Therm Anal Calor* **2014**, *115*, 1119-1125. DOI10.1007/s10973-013-3438-z.

12. Muraleedharan, K.; Kripa, S. DSC kinetics of the thermal decomposition of copper(II) oxalate by isoconversional and maximum rate (peak) methods. *J Therm Anal Calor* **2014**, *115*, 1969-1978. DOI10.1007/s10973-013-3366-y.

13. Hartman, K. O. The kinetics of oxalate ion pyrolysis in a potassium bromide matrix. *J. Phys. Chem.* **1967**, *71*, 392-396.

14. Degen, J.; Schmidtke, H. -.; Stoyanova, R.; Angelov, S.; Atanasov, M. Emission spectra of CO2 - radicals, stabilized in SrCO3 obtained by thermal decomposition of SrC2O4·H2O. *Chem. Phys.* **1990**, *147*, 415-420. DOI10.1016/0301-0104(90)85055-2.

15. Kolezynski, A.; Malecki, A. Theoretical studies of electronic structure and structural properties of anhydrous alkali metal oxalates: Part II. Electronic structure and bonding properties versus thermal decomposition pathway. *J Therm Anal Calor* **2014**, *115*, 841-852. DOI10.1007/s10973-013-3210-4.

16. Wladimirsky, A.; Palacios, D.; D'Antonio, M.C.; Gonzalez-Baro, A.C.; Baran, E.J. Vibrational Spectra of the α-$M^{II}C_2O_4$*$2H_2O$ Oxalato Complexes, with M^{II}=Co, Ni, Zn. J. Argent. Chem. Soc., 2011, 98, 71-77.

17. Vlaev, L.; Nedelchev, N.; Gyurova, K.; Zagorcheva, M. A comparative study of non-isothermal kinetics of decomposition of calcium oxalate monohydrate. *J. Anal. Appl. Pyrolysis* **2008**, *81*, 253-262. DOI10.1016/j.jaap.2007.12.003.

18. Vyazovkin, S.; Burnham, A. K.; Criado, J. M.; Pérez-Maqueda, L. A.; Popescu, C.; Sbirrazzuoli, N. ICTAC Kinetics Committee recommendations for performing kinetic computations on thermal analysis data. *Thermochim Acta* **2011**, *520*, 1-19. DOI10.1016/j.tca.2011.03.034.

19. Starink, M. J. A new method for the derivation of activation energies from experiments performed at constant heating rate. *Thermochim Acta* **1996**, *288*, 97-104.